

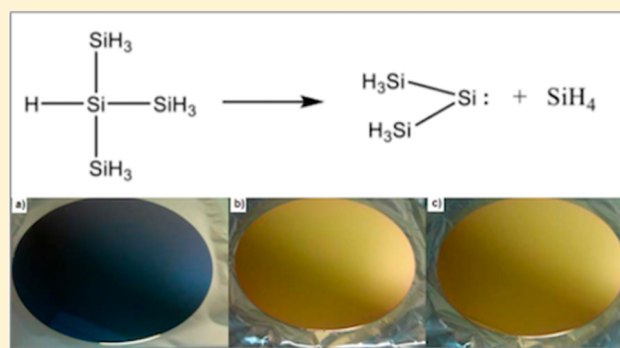
Synthesis and Exploratory Deposition Studies of Isotetrasilane and Reactive Intermediates for Epitaxial Silicon

Barry Arkles,^{*,†} Youlin Pan,[†] Fernando Jove,[†] Jonathan Goff,[†] and Alain Kaloyeros[‡]

[†]Gelest Inc., Morrisville, Pennsylvania 19067, United States

[‡]SUNY Polytechnic Institute, Albany, New York 12203, United States

ABSTRACT: A synthetic method is presented for the production of isotetrasilane, a higher order perhydrosilane, with the purity and volume necessary for use in extensive studies of the chemical vapor deposition (CVD) of epitaxial silicon (e-Si) thin films. The chemical characteristics, thermodynamic properties, and epitaxial film growth of isotetrasilane are compared with those of other perhydrosilanes. A film-growth mechanism distinct from linear perhydrosilanes $H(SiH_2)_nH$, where $n \leq 4$, is reported. Preliminary findings are summarized for CVD of both unstrained e-Si and strained e-Si doped with germanium (Ge) and carbon (C) employing isotetrasilane as the source precursor at temperatures of 500–550 °C. The results suggest that bis-(trihydrosilyl)silylene is the likely deposition intermediate under processing conditions in which gas-phase depletion reactions are not observed.



under processing conditions in which gas-phase depletion

INTRODUCTION

As emerging integrated chip (IC) and solar cell technologies continue to reduce individual device feature sizes, chemical vapor deposition (CVD) of epitaxial silicon (e-Si) has emerged as a critical enabling step in achieving the desired architectures and performance.^{1–3} In particular, CVD of e-Si has become an essential building block for improving performance in strained p-type metal oxide semiconductor field effect transistors (p-MOSFETs) by increasing the concentration of embedded germanium (Ge) in the Si matrix.⁴ This effect is attributed to increased hole mobility due to the biaxial compressive strain caused by the introduction of Ge into the Si host matrix.

Further strain enhancement in the embedded SiGe (e-SiGe) system is still required with decreasing feature size due to disproportionate reduction in device area caused by nonscaled gate length.⁵ This enhancement is typically achieved by further increasing Ge concentrations in Si to levels as high as 45%.⁶ However, in light of the lattice mismatch between Si and Ge, thermally induced relaxation of the e-SiGe matrix during epitaxial growth and subsequent device fabrication steps is a major concern, as the elevated deposition and processing temperatures associated with these steps may cause structural defects in e-SiGe materials with high Ge concentration, such as stacking faults and misfit dislocations.⁷

This issue has plagued conventional CVD e-Si, which employs lower order silanes, such as silane or disilane as Si sources, due to the need for deposition temperatures in excess of 700 °C to achieve adequate growth rates. Some efforts to reduce the thermal budget below 600 °C in order to eliminate structural defects employed higher order perhydrosilanes

such as trisilane. However, the latter was observed to generate gas-phase particles (silicon hydride clusters) due to its much higher reactivity and lower dissociation energy in comparison to silane and disilane.⁵ It was therefore necessary to lower the partial vapor pressure of trisilane in the reaction zone during the deposition process, again resulting in an undesirable reduction in growth rates.⁷

Further research activities examined the CVD growth of e-Si from neopentasilane ($H_{12}Si_5$), as the Si precursor. Chung et al. and Sturm et al. used neopentasilane to achieve e-Si growth rates of 215, 130, and 54 nm/min at substrate temperatures of 700, 650, and 600 °C, respectively.^{8,9} Chung et al. also reported the formation of C-doped e-Si ($Si_{1-y}C_y$) using neopentasilane and methylsilane (CH_3SiH_3) as Si and C sources, respectively, with the highest C substitution level being 2.1%.⁸ Similarly Koo et al. demonstrated the deposition of good e-Si film quality from *n*-tetrasilane ($H_{10}Si_4$).¹⁰ However, the lower limit of the e-Si deposition window at acceptable growth rates was 600 °C for both neopentasilane and *n*-tetrasilane. Attempts to grow e-Si by CVD from *n*-tetrasilane at substrate temperatures below 600 °C yielded very low growth rates and/or an amorphous Si film.¹¹

Given the drive to realize e-Si CVD growth at temperatures below 600 °C and the achievement of higher Ge or C substitution levels in the e-Si matrix, a number of investigators have proposed another higher order perhydrosilane: isotetrasilane (Si_4H_{10}).^{5,7,10,12} A literature search for “iso-

Received: October 24, 2018

Published: February 20, 2019

tetrasilane and deposition” on Scifinder found more than 30 patents in which the utility of isotetrasilane has been predicted but not demonstrated. This report presents a summary of experimental details pertaining to the synthesis of isotetrasilane, CVD processing parameters, and precursor and film characterization techniques. An analysis comparing the properties, decomposition characteristics, deposition behavior, and advantages of isotetrasilane versus other Si source chemistries is provided. Results from an exploratory low-temperature CVD (LTCVD) study of unstrained and strained e-Si using isotetrasilane as the Si source at 500 °C demonstrates conformal deposition of silicon under conditions consistent with semiconductor manufacturing.

RESULTS AND DISCUSSION

Synthesis of Pure Isotetrasilane. While the earliest literature on hydridosilanes authored by Stock¹³ observed isotetrasilane as part of a mixture, a practical synthesis which allows isolable material has not been previously reported. Rather, the properties for isotetrasilane reported in the literature are extrapolations from an isomeric mixture.¹⁴ One objective of the work reported here was to develop a practical synthesis of isotetrasilane of sufficient quantity and purity to carry out exploratory CVD studies, including analyses of its decomposition characteristics. As part of a systematic approach for the scalable synthesis of isotetrasilane, it was considered desirable to generate a stable, nonpyrophoric intermediate high in both purity and yield. Tris(trichlorosilyl)silane was selected for that purpose, the synthesis protocol for which is based upon a method reported earlier.¹⁵

Preparation of Tris(trichlorosilyl)silane. The cleavage reaction of tetrakis(trichlorosilyl)silane leading to the preparation of tris(trichlorosilyl)silane is shown schematically in Figure 1. Although yields of this intermediate were only in the

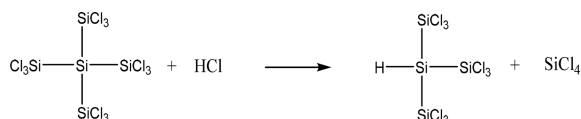


Figure 1. Chemical reaction leading to the preparation of tris(trichlorosilyl)silane.

range of 65–75%, the stability and nonpyrophoric nature of the material were deemed acceptable for larger-scale reduction. More information about this intermediate, as well as other perchlorinated oligosilanes, can be found in the recent review article by Teichmann et al.¹⁶

Preparation of Isotetrasilane. The reduction of tris(trichlorosilyl)silane to isotetrasilane is shown in Figure 2. The reduction was conducted in a high-boiling solvent, a C₁₀ alkylated aromatic that enabled the separation of the more volatile isotetrasilane. Diisobutylaluminum hydride was preferred as the reductant over lithium aluminum hydride, since the latter generated small quantities of pyrophoric lower



Figure 2. Chemical reduction of tris(trichlorosilyl)silane leading to isotetrasilane.

silanes, which were problematic from a safety and handling perspective.

Large-Scale (Industrial) Preparation of Isotetrasilane and Observation of Bis(trihydrosilyl)silylene. The synthetic apparatus used in the large-scale (industrial) synthesis of isotetrasilane is depicted in Figure 3. Due to the pyrophoric nature of both isotetrasilane and potential by-products, a controlled system was constructed to allow the production of crude isotetrasilane with the ability to operate under tight engineering control. Prior to operation, the system was leak-checked by pressurizing it with helium and monitoring its ambient pressure with a residual gas analyzer (RGA). The core reactor, shown schematically in section ii of Figure 3, was a double-gasketed stainless steel-jacketed reactor with a nominal capacity of 19 L. The reactor was equipped with a heating and cooling control unit, magnetically coupled air-drive agitator, thermocouple probe, metering pump, and 45 mm unpacked column outfitted with a condenser. Transport of the crude product was made through double-walled stainless steel tubing plumbed directly to a separate distillation apparatus for final purification. Essential to a safe design is venting through an oxidizing scrubber with a flash-back preventer. The physical properties as determined for isotetrasilane are provided in Table 2. It should be noted that the MS fragment of m/z 90 is $M^+ - \text{SiH}_4$, which shows that the fragment $(\text{SiH}_3)_2\text{Si}$: (bis(trihydrosilyl)silylene) is quite stable, given that its intensity is 100%.

CVD Processing Parameters and Film Characterization Techniques. Experimental details pertaining to CVD processing parameters and resulting film characterization techniques have already been reported and will be summarized herein.^{5,7} Deposition experiments were carried out in a 300 mm single-wafer industrial CVD system on both blanket and Si oxide/Si nitride patterned Si (001) substrates with light p doping (resistance 7–10 Ω/cm). Isotetrasilane, methylsilane (CH₃SiH₃), phosphine (PH₃), and germane (GeH₄) were employed as source precursors for Si, C, P, and Ge, respectively. All experiments were carried at substrate temperatures in the range 500–550 °C and reactor working pressures of 10–100 Torr. Hydrogen was used as the carrier gas at 10000 sccm flow rate. The resulting growth rates were constant at 10 nm/min.

Comparative Analysis of the Chemical Properties of Isotetrasilane versus Conventional Si Source Chemistries. In the case of CVD of e-Si, the differences in structure, composition, and performance of the resulting e-Si films can largely be attributed to the fundamental chemical and thermodynamic properties of the Si source precursors. In this context, Table 1 lists the source chemistries that have been used most commonly as Si sources in CVD e-Si. The intent is to provide a baseline comparison of bond dissociation energies and chemical structures with isotetrasilane. In particular, it should be noted that isotetrasilane exhibits more advantageous chemical properties in comparison to neopentasilane, especially in terms of its much higher vapor pressure of 35 Torr at 22 °C versus 15 Torr at 25 °C. Table 2 summarizes relevant properties of these Si source precursors reported earlier in the literature and includes new data for isotetrasilane and neopentasilane determined as part of these studies. Table 2 reports data for perhydrosilanes containing up to five silicon atoms that are viable candidates for CVD applications, as they satisfy the following basic requirements: (i) they are stable during storage, transition, and handling; (ii) they are

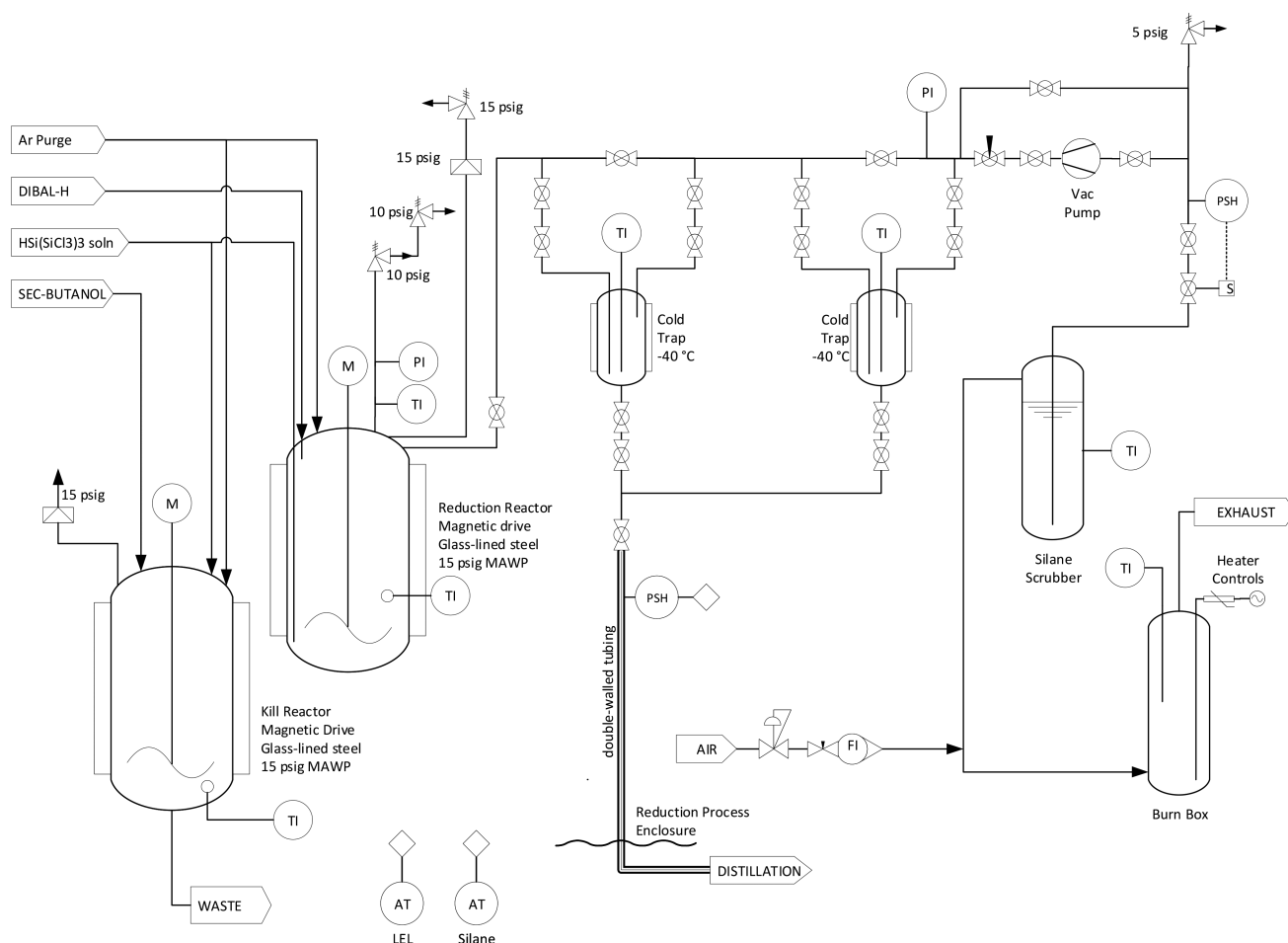


Figure 3. Simplified schematic depiction of the actual large-scale (industrial) system used in the preparation of isotetrasilane. The overall system consists of seven sections with all connections welded or VCR fittings: (i) inert gas supply manifold; (ii) the primary reactor section (depicted); (iii) the nonvolatile input and output (depicted); (iv) support utilities; (v) product output and traps (depicted); (vi) vacuum system and pyrophoric byproduct abatement (depicted); (vii) crude product final distillation and analysis.

readily vaporized; (iii) they exhibit vapor pressures conducive to straightforward transport to the reaction zone while their integrity is maintained. Furthermore, given their higher vapor pressure, perhydridosilanes containing up to five Si atoms can be delivered under vacuum conditions to a deposition chamber without a carrier gas.

The general literature on resulting film characteristics suggests that isotetrasilane has significant potential to yield high-quality tensile and compressive strained Si. Theoretical and empirical mechanistic pathway studies that support this suggestion broadly cover three areas of analysis: (i) reactive intermediates in the vapor phase, (ii) substrate surface-driven intermediates, and (iii) surface decomposition and role of sticking coefficient. More specifically, theoretical studies have focused on thermal decomposition routes of isotetrasilane, including the evolution and stabilization of intermediate radicals in the gas phase and at the interface with the substrate surface.^{17,18} As noted by Swihart and co-workers, the decomposition steps of isotetrasilane involve four types of reactions: (i) homolytic dissociation, (ii) 1,2-H shift, (iii) 1,3-H shift, and (iv) H₂ elimination. In the case of both disilane and neopentasilane, 1,2-H shift reactions only produce simple silylene due to the more symmetrical chemical structure of the parent molecule. In contrast, 1,2-H shift reactions for trisilane and isotetrasilane lead to a more diverse product spectrum.¹⁹

Swihart notes that the relatively low free energies associated with gaseous cluster formation suggest thermodynamic pathways that lead to gas-phase depletion reactions and, ultimately, formation of particles in the gas phase.^{5,7} The latter are believed to be caused by the occurrence of ring systems due to cyclization, leading to the manifestation of gas-phase clusters (nanoparticles) which consist of neutral or negatively charged hydrogenated silicon compounds.

Nonlinear (branched) perhydridosilanes containing five or fewer Si atoms are less likely to form ring systems by cyclization in comparison to linear perhydridosilanes containing the same number of Si atoms, in part due to the ring strain associated with these systems and also because the probability for gas-phase insertion of silylene into branched perhydridosilanes is expected to be lower than that of linear perhydridosilanes. Given the substantially different bond energies between Si–Si and Si–H bonds, simultaneous scission of both types of bonds is less likely at the deposition temperatures reported herein.

It should also be noted that the electron affinities of the linear and branched structures of the silylene intermediates of *n*-tetrasilane and isotetrasilane decomposition have been calculated to be 1.84 and 2.07 eV, respectively²⁰—values that imply a high threshold for particle formation. Formation of silylenes occurs at temperatures of ~300 °C and is relatively

Table 1. Si–Si and Si–H Bond Dissociation Energies for Selected Si Chemistries^{25–27}

Source		Bond Dissociation Energy (kJ/mole)	Structure
Name	Formula		
Silane	SiH ₄ (Si-H)	384	
Disilane	Si ₂ H ₆ (Si-H)	374	
	Si ₂ H ₆ (Si-Si)	321	
Trisilane	Si ₃ H ₈		
	terminal Si-H	363	
	internal Si-H	353	
Tetrasilane	Si ₄ H ₁₀		
	terminal Si-H	363	
	internal Si-H	353	
	terminal Si-Si	297	
	internal Si-Si	284	
	(SiH ₃) ₃ SiH		
terminal Si-H	363		
internal Si-H	343		
	(SiH ₃) ₃ SiH (Si-Si)	297	
	(SiH ₃) ₄ Si (Si-H)	363	
(SiH ₃) ₄ Si (Si-Si)	297		

Table 2. Relevant Properties of Pertinent Si Source Precursors⁴

perhydrosilane	formula	boiling point, °C	melting point, °C	vapor pressure, °C (Torr)	density	refractive index
silane	SiH ₄	-112	-185	20 (>760)	0.680	
disilane	Si ₂ H ₆	-14.5	-132	21.1 (2586)	0.686	
trisilane	Si ₃ H ₈	52.9	-117	0 (95.5)	0.743	
<i>n</i> -tetrasilane	Si ₄ H ₁₀	106	-85 to -95	20 (22)	0.825	
isotetrasilane	Si ₄ H ₁₀	101	-99	35 (22)	0.793	1.5449 ²⁰
neopentasilane	Si ₅ H ₁₂	132–134	←40	25 (15)	0.805	1.5604 ²⁵

⁴Isotetrasilane and neopentasilane data were determined by the authors. Comparative data for other compounds are taken from the literature.^{13–15}

stable in high-energy environments, as evidenced by GC-MS, which utilizes 70 eV for ionization.²¹ Other intermediates that form at elevated temperature, presumably generated by homolytic cleavage of Si–Si bonds, are less stable and are probable intermediates for gas-phase depletion reactions.

Substrate surface-initiated intermediate formation and film growth occur through a number of mechanisms. However, key variations in the underlying adsorption mechanisms at the interface with the substrate are of particular note in differentiating the deposition paths of the various perhydrosilanes. These variations are driven by the relative availability of Si atoms with bonds to three hydrogens. It has been demonstrated that trihydrosilanes undergo a reactive adsorption with release of hydrogen and formation of a substituted silylene radical on a variety of substrates, including Si(100).^{22,23}

Branched perhydrosilanes such as isotetrasilane necessarily have a greater proportion of Si atoms bonded to three

hydrogens in comparison their linear analogues. They are therefore more likely to undergo dissociative adsorption at the interface with the substrate. In this respect, it was shown that the sticking coefficient ϵ , defined as the number of adsorbed molecules per number of impacts, increased with Si content in the precursor as follows:

$$\epsilon(\text{SiH}_4) = 1.5 \times 10^{-6} < \epsilon(\text{Si}_2\text{H}_6) = 6.3 \times 10^{-5} < \epsilon(\text{Si}_3\text{H}_8) \approx 3 \times 10^{-4}$$

These observations are supported by experimental gas-phase kinetic studies of the absolute reactivity of silane chemistries, as reported by Jasinski.²⁴ These studies employed an array of in situ analytical tools, including flash photolysis with laser absorption, laser-induced fluorescence (LIF), laser magnetic resonance (LMR), photoionization mass spectrometry, resonance enhanced multiphoton ionization (REMPI), and low-energy electron impact ionization mass spectrometry. Most notably, Jasinski reported that monosilicon hydride radicals (such as SiH and SiH₂) are highly reactive with Si–H bonds in

silane and concluded that the diffusion probability of such species from the gas phase to the substrate surface in CVD processes is negligible. Instead, silyl (H_3Si^*) is the dominant gas phase radical in plasma CVD at steady state and therefore easily reaches the substrate surface. Alternatively, silylene is the most likely gas-phase species to be formed in thermal CVD processes and is therefore the predominant species in substrate surface adsorption and decomposition mechanisms.

However, these theoretical studies do not consider the nonradical formation of a silylene by reductive elimination of silane. The likely significant intermediate in isotetrasilane decomposition is (i) bis(trihydrosilyl)silylene ($(\text{H}_3\text{Si})_2\text{Si}$), a species formed by a reductive elimination mechanism generating silane as a byproduct as shown below. This possible decomposition pathway (Figure 4) is proposed by the authors

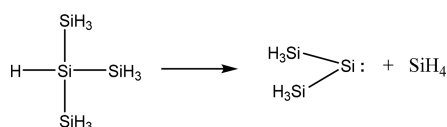


Figure 4. Reductive elimination of silane from isotetrasilane to form bis(trihydrosilyl)silylene.

as a probable explanation for an alternate film growth mechanism observed in our exploratory CVD studies of isotetrasilane and not observed in other linear perhydrosilanes with silicon atom numbers ≤ 4 .

The theoretical and empirical studies summarized above support the proposition that isotetrasilane is a superior candidate for CVD e-Si than its lower order perhydrosilane counterparts. Potential advantages of isotetrasilane that are particularly noteworthy are (i) reduced particle formation in the reaction zone due to the inhibition of undesirable gas-phase reactions and (ii) lower decomposition temperature due in part to its higher surface sticking coefficient. Given these advantages, it would be logical to assume that isotetrasilane has been the subject of extensive film deposition studies. Curiously, however, a literature search for “isotetrasilane and deposition” on Scifinder found prophetic uses of isotetrasilane in over 30 patents, but not a single report on the actual use of isotetrasilane in CVD studies.

Comparative CVD e-Si Results from Isotetrasilane versus Lower Order Perhydrosilanes. The focus of the CVD scoping studies summarized herein is 2-fold: (1) to compare CVD e-Si results from isotetrasilane versus lower order perhydrosilanes and (2) to report findings from exploratory CVD e-SiGe (>30 atom % Ge) and CVD e-SiC (>2.4 atom % C) thin film structures.

Our overall findings support the theoretical and empirical investigations of gas-phase and surface reaction pathways discussed earlier, which underline the chemical decomposition routes of isotetrasilane and lead to the deposition of e-Si at a significantly reduced temperature and higher growth rates in comparison to lower order perhydrosilanes. The data in Table 3 shows that the use of isotetrasilane as the source precursor yielded CVD e-Si films in the temperature range of 500–550 °C, well below the 600–750 °C reported for lower order perhydrosilanes. As can also be seen in Table 3, and as suggested by Chung et al.,¹² isotetrasilane exhibits two different growth rate mechanisms: a faster growth rate process that displays gas-source depletion at temperatures as low as 550 °C and a working pressure of 100 Torr and a gas-phase depletion-free process with relatively slower growth rate values of 13 and 43 nm/min at 550 and 600 °C, respectively. Chung et al. observed that decreasing the reaction working pressure or lowering the deposition temperature eliminated gas-phase depletion phenomena.¹² The gas-phase depletion-free process was considered by Chung to be due not to the formation of silane or disilane reaction byproducts but rather to the formation of a slower reacting isomer or a higher-order silane byproduct, such as trisilane.

The isotetrasilane decomposition profile reported in Table 3, and the work of Chung et al. are instead consistent with the formation of the bis(trihydrosilyl)silylene intermediate in the reductive elimination mechanism of isotetrasilane. The GC-MS data (70 eV ionization) shows nearly quantitative formation of silane as well as the mass ion associated with bis(trihydrosilyl)silylene. Bis(trihydrosilyl)silylene appears to act as the effective intermediate for epitaxial deposition of Si. This finding is supported by prior theoretical and experimental studies regarding gas-phase reactions and substrate surface adsorption and decomposition mechanisms of silanes,

Table 3. Selected Comparative Results from Exploratory CVD e-Si from Isotetrasilane

precursor	temp (°C)	working pressure (Torr)	growth rate (nm/min)	gas-phase depletion/particle formation
silane ^a	650	80	11	no
silane ^a	750	100	97	yes, gas-phase depletion
disilane ^a	650	100	18	no
disilane ^a	700	100	28	yes, gas-phase depletion
trisilane ⁷	550	10	10	yes, gas-phase particle formation
<i>n</i> -tetrasilane ^a	600	100	<10	no
<i>n</i> -tetrasilane ⁷	550	10	10	yes, gas-phase particle formation
<i>n</i> -tetrasilane ²⁸	550	0.0525×10^{-3}	2	no
<i>n</i> -tetrasilane ¹¹	550	N/A	N/A	no, however, the Ge concentration in e-SiGe was limited to $\cong 12\%$
neopentasilane ²⁹	550	6	~ 18	no
isotetrasilane ^a	550	100	13	yes, gas-phase depletion
isotetrasilane ^a	550	40	26	yes, gas-phase depletion
isotetrasilane ^a	550	10	35	no
isotetrasilane ^a	525	100	18	yes, gas-phase depletion
isotetrasilane ^a	500	100	12	no

^aData provided in this table were produced as part of a collaboration among Gelest, IBM, Matheson TriGas, and SUNY Polytechnic Institute, as acknowledged. Comparative data were compiled from the literature noted within the table.

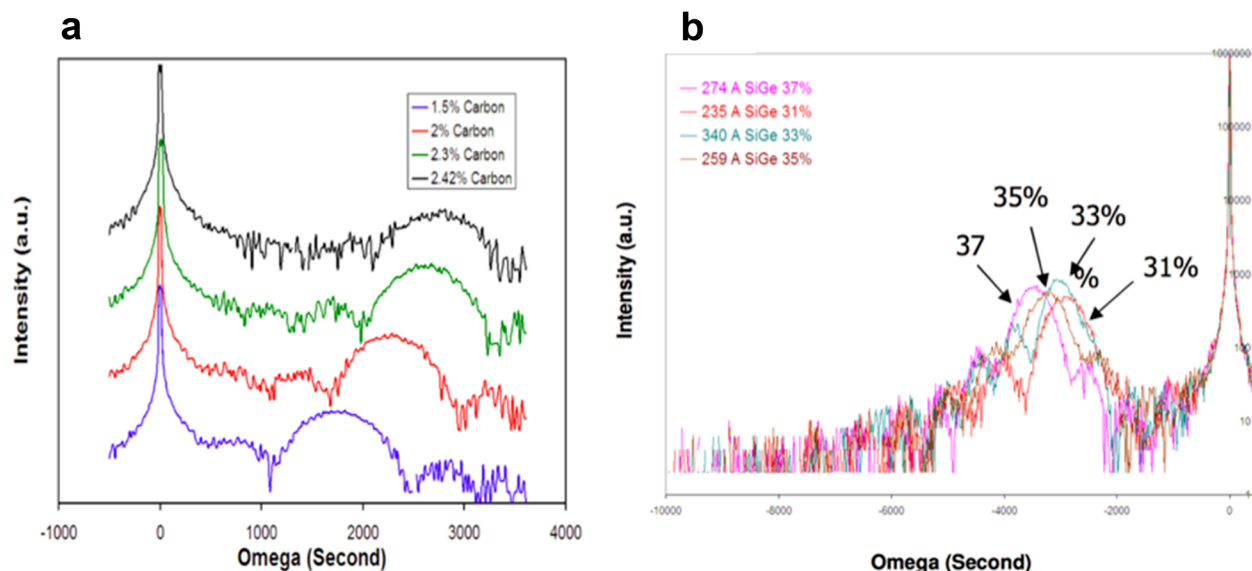


Figure 5. XRD patterns for strained CVD e-Si (both compression and tensile strain) films grown at 550 °C by (a) codeposition from isotetrasilane and methylsilane as Si and C source precursors, respectively, and (b) codeposition from isotetrasilane and germane as Si and Ge sources, respectively.

including the extensive reports by Swihart and co-workers and Jasinski, as discussed earlier.^{18,20,24}

Exploratory CVD e-SiGe (>30 atom % Ge) and CVD e-Si:C (>2 atom % C) Thin Film Studies. Figure 5a displays X-ray diffraction (XRD) patterns for strained CVD e-SiGe (both compression and tensile strain) films grown at 550 °C by codeposition from isotetrasilane and germane as Si and Ge sources, respectively. XRD profiles demonstrate that up to 37% Ge was successfully incorporated into the e-Si matrix at 550 °C at film thicknesses ranging from 26 to 340 nm. Similarly, Figure 5b depicts X-ray diffraction (XRD) patterns for strained CVD e-Si:C (both compression and tensile strain) films grown at 550 °C by codeposition from isotetrasilane and methylsilane as Si and C sources, respectively. XRD profiles indicate that up to 2.4% C was successfully incorporated into the e-Si matrix at 550 °C at film thicknesses equivalent to those reported above for e-SiGe. The XRD findings were supported by AFM, TEM, and SIMS analyses that confirmed the XRD data presented herein. The data in Table 3 demonstrate the advantages of using isotetrasilane as the Si source precursor in terms of its capability to grow high-quality e-Si at significantly lower temperatures and higher growth rates in comparison to neopentasilane and *n*-tetrasilane and, as a result, the ability to embed higher levels of elements such as Ge and C in the e-Si matrix.

CONCLUSIONS

A practical, scalable synthesis for isotetrasilane has been demonstrated and employed in exploratory CVD studies of e-Si. Epitaxial deposition of both compressive and tensile strained silicon was demonstrated, with optimum deposition achieved at temperatures in the range of 500–550 °C. Gas-phase depletion reactions were suppressed at lower temperatures and lower partial pressures. It is clear from these exploratory studies that a film-growth mechanism exists for isotetrasilane at temperatures of less than 550 °C at pressures <40 Torr and at temperatures of less than 500 °C at pressures up to 100 Torr that is distinct from that of the linear perhydrosilanes studied. The deposition behavior is con-

sistent with the formation of bis(trihydrosilyl)silylene, which the authors propose is formed by the reductive elimination of silane from isotetrasilane.

EXPERIMENTAL SECTION

Materials, Methods, and Instrumentation. Tetrakis-(trichlorosilyl)silane was obtained from Gelest Inc. Alkylated benzene (C₁₀ aromatics) was purchased from Exxon. Density and refractive index (AO ABBE refractor Model 10450) were determined in a Braun glovebox. ¹H NMR and ²⁹Si NMR spectra were obtained using a Bruker 400 MHz NMR spectrometer. NMR samples were diluted to 10 vol % in deuterobenzene.

Amorphous and polycrystalline Si layers were deposited on 100 nm wet oxide using a 300 mm single-wafer industrial reduced-pressure chemical vapor deposition (RPCVD) tool. Deposition was conducted under a fixed hydrogen flow rate of 10 slpm. Optical pyrometry was used to measure the temperature, calibrated using a National Institute of Standards and Technology (NIST) thermocouple wafer. Film thickness, morphology, and composition were determined by X-ray diffraction on a BEDE Metrix-L X-ray tool from Jordan Valley Semiconductors, tapping mode atomic force microscopy (AFM) using a DI3100 Nanoscope IV instrument, transmission electron microscopy (TEM) on a Phillips CM20 TEM apparatus, and secondary ion mass spectrometry (SIMS) on a Physical Electronics ADEPT-1010 quadrupole SIMS instrument.

Preparation of Tris(trichlorosilyl)silane. A 5658.0 g portion (10 mol) of perchloroneopentasilane and 7650 mL of tetrachlorosilane solvent were charged to a 22 L, four-neck flask equipped with a mechanical stirrer, a pot thermometer, a funnel, and a nitrogen-protected dry ice condenser. The reaction mixture was heated to 40–50 °C with stirring until the perchloroneopentasilane was completely dissolved in the tetrachlorosilane. The mixture was subsequently cooled to room temperature, during which formation of solids was observed. A 4500 mL portion of 2 M anhydrous HCl in ether was added to the stirred reaction mixture over a 4 h period, while the pot was maintained at room temperature. The cloudy reaction mixture turned to a clear solution after the HCl addition, and GC-MS confirmed formation of the desired product in the mixture. Distillation was used for purification. Tetrachlorosilane was removed at atmospheric pressure without allowing the pot temperature to exceed 80 °C. A 2512.7 g amount (70% yield) of the desired product, tris(trichlorosilyl)silane, was obtained at 60–62 °C at 0.2 Torr. Tris(trichlorosilyl)silane is a colorless liquid. ²⁹Si{¹H} NMR (400

MHz, C_6D_6): δ -23.8 (-SiCl₃), -109 ppm (-SiH). MS: m/z 396.7 ($M - Cl^+$, 8%), 90 ($M - SiCl_3^+$, 42%).

Small-Scale Preparation of Isotetrasilane. A 100 mL, four-neck flask equipped with a magnetic stirrer, a pot thermometer, an addition funnel, and a short glass helix packed column was charged with 7.21 g (0.017 mol) of tris(trichlorosilyl)silane and 7.21 g of alkylated benzene (C_{10} aromatics). The entire system was degassed and backfilled twice with argon. The mixture was cooled to 5 °C, and 23.70 g (0.17 mol) of diisobutylaluminum hydride was added to the mixture over a 4 h period, with the pot temperature maintained between 10 and 40 °C. Upon completion of the addition of diisobutylaluminum hydride, the pot mixture was heated to 50 °C for 2 h. Crude product was then distilled at a pot temperature below 65 °C under reduced pressure (3 mmHg) over 6–8 h period. Redistillation gave 1.14 g (56% yield) of isotetrasilane with a purity of 99.1%. Isotetrasilane is a pyrophoric, colorless liquid; bp 101–102 °C, mp -99 °C. ¹H NMR (400 MHz, C_6D_6): δ 2.73 (br s, 1H), 3.35 ppm (s, 9H). ²⁹Si NMR (400, C_6D_6): δ -90.6, -93.1, -95.7, -98.1 (-SiH₃); -135.7, -138.1 ppm (-SiH). MS: m/z 122 (M^+ , 8%), 90 ($M^+ - SiH_4$, 100%).

Large (Industrial)-Scale Preparation of Isotetrasilane. Under an argon atmosphere, the reactor was charged with 1837.7 g (4.25 mol) of tris(trichlorosilyl)silane and 1721.2 g of alkylated benzene (C_{10} aromatics). The entire system was degassed and backfilled twice with argon. The mixture was subsequently cooled to 5 °C, and 5620.8 g (39.53 mol) of diisobutylaluminum hydride was added over 4 h via a metering pump, with the temperature maintained between 10 and 40 °C. When the addition of diisobutylaluminum hydride was complete, the reactor was heated to 50 °C and held at this temperature for 2 h. Crude product was separated from the reaction mixture by flash distillation through a 45 mm diameter × 75 cm tall unpacked column, the temperature in the reaction vessel being maintained below 65 °C with 3 Torr over a 6–8 h period. The crude product had a nominal purity of >90%. The reaction pot mixture (depleted of isotetrasilane) was separately transferred to a 75 L jacketed reactor equipped with a flash-back preventer, where it was cooled to 10 °C and purged with argon before *sec*-butanol was added over a period of 3 h. The mixture was then purged with air for 30 min and stirred for an additional 4 h. The pyrophoric potential of the byproduct mixture was thus fully abated and could be disposed of safely. All effluent gas streams were passed through an argon-blanketed counter-current scrubber with a KOH/NaOH contact solution, before passing to a thermal oxidizer (silane burn box). Redistillation of the crude product through a glass helix packed column gave 410.3 g (~60% yield) of the title compound with a purity of 99.3%. (Note: the primary impurity is alkylated aromatics; minor impurities, as inferred by GC-MS, include disiloxane, trisilane, *n*-tetrasilane, and pentasilane isomers.)

Caution! This synthesis deals with pyrophoric materials. Diisobutylaluminum hydride ignites on exposure to air. Isotetrasilane ignites instantaneously on exposure to air, typically with audible report. The handling of these materials under atmospheric or greater than atmospheric pressure is dangerous. The handling of these materials under subatmospheric conditions has even greater hazard potential, since the failure of seals with ingress of air can lead to explosions. For this reason subatmospheric reaction or transfer equipment should be double-gasketed or double-walled, with the primary seal monitored for failure. Equipment should be designed to consider the potential to generate small amounts of noncondensable pyrophoric byproducts such as silane.

AUTHOR INFORMATION

Corresponding Author

*E-mail for B.A.: Executiveoffice@gelest.com.

ORCID

Barry Arkles: 0000-0003-4580-2579

Jonathan Goff: 0000-0002-4794-1356

Notes

The authors declare no competing financial interest.

ACKNOWLEDGMENTS

The authors acknowledge their collaborators Thomas Adam, Paul Brabant, Terry Francis, Devendra Sandana, Manabu Shinriki, and Keith Chung, who performed the deposition studies in a collaborative program at SUNY Polytechnic University—Albany Nanotechnology Center, under a joint research and development (R&D) program among IBM, Matheson TriGas, and Gelest.

REFERENCES

- (1) Lukianov, A.; Ihara, M. Free-Standing Epitaxial Silicon Thin Films for Solar Cells Grown on Double Porous Layers of Silicon and Electrochemically Oxidized Porous Silicon Dioxide. *Thin Solid Films* **2018**, *648*, 1–7.
- (2) Hens, P.; Brow, R.; Robinson, H.; Cromar, M.; Van Zeghbroeck, B. Epitaxial Growth of Cubic Silicon Carbide on Silicon Using Hot Filament Chemical Vapor Deposition. *Thin Solid Films* **2017**, *635*, 48–52.
- (3) Branz, H. M.; Teplin, C. W.; Romero, M. J.; Martin, I. T.; Wang, Q.; Alberi, K.; Young, D. L.; Stradins, P. Hot-Wire Chemical Vapor Deposition of Epitaxial Film Crystal Silicon for Photovoltaics. *Thin Solid Films* **2011**, *519* (14), 4545–4550.
- (4) Vincent, B.; Vandervorst, W.; Caymax, M.; Loo, R. Influence of Si Precursor on Ge Segregation during Ultrathin Si Reduced Pressure Chemical Vapor Deposition on Ge. *Appl. Phys. Lett.* **2009**, *95* (26), 262112.
- (5) He, H.; Brabant, P.; Chung, K.; Shinriki, M.; Adam, T.; Reznicek, A.; Sadana, D.; Hasaka, S.; Francis, T. High Strain Embedded-SiGe via Low Temperature Reduced Pressure Chemical Vapor Deposition. *Thin Solid Films* **2012**, *520*, 3175–3178.
- (6) Tamura, N.; Shimamune, Y. 45nm CMOS Technology with Low Temperature Selective Epitaxy of SiGe. *Appl. Surf. Sci.* **2008**, *254*, 6067.
- (7) Shinriki, M.; Chung, K.; Hasaka, S.; Brabant, P.; He, H.; Adam, T. N.; Sadana, D. Gas Phase Particle Formation and Elimination on Si (100) in Low Temperature Reduced Pressure Chemical Vapor Deposition Silicon-Based Epitaxial Layers. *Thin Solid Films* **2012**, *520* (8), 3190–3194.
- (8) Chung, K. H.; Sturm, J. C.; Sanchez, E.; Singh, K. K.; Kuppuraio, S. The High Growth Rate of Epitaxial Silicon-Carbon Alloys by Using Chemical Vapor Deposition and Neopentasilane. *Semicond. Sci. Technol.* **2007**, *22* (1), S158.
- (9) Sturm, J.; Chung, K. Chemical Vapor Deposition Epitaxy of Silicon-Based Materials Using Neopentasilane. *ECS Trans* **2008**, *16* (10), 799–805.
- (10) Koo, S.; Jang, H.; Ko, D.-H. Epitaxy of Si 1-x C x via Ultrahigh-Vacuum Chemical Vapor Deposition Using Si 2 H 6, Si 3 H 8, or Si 4 H 10 as Si Precursors. *Jpn. J. Appl. Phys.* **2017**, *56* (9), 095502.
- (11) Hart, J.; Hazbun, R.; Eldridge, D.; Hickey, R.; Fernando, N.; Adam, T.; Zollner, S.; Kolodzey, J. Tetrasilane and Digermane for the Ultra-High Vacuum Chemical Vapor Deposition of SiGe Alloys. *Thin Solid Films* **2016**, *604*, 23.
- (12) Chung, K. H.; Brabant, P.; Shinriki, M.; Hasaka, S.; Francis, T.; He, H.; Sadana, D. K. Gas Source Depletion Study of High-Order Silanes of Silicon-Based Epitaxial Layers Grown with RPCVD and Low Temperatures. *ECS Trans.* **2012**, 4569.
- (13) Stock, A. *Hydrides of Boron and Silicon*; George Fisher Baker non-resident lectureship in chemistry at Cornell University; Cornell University Press: 1933.
- (14) Gokhale, S. D.; Jolly, W. L. Some Properties of *n* and Isotetrasilane. *Inorg. Chem.* **1964**, *3* (7), 946–949.
- (15) Arkles, B. C.; Pan, Y. Trihydrosilyl-Terminated Polysilanes and Methods of Preparation. US Pat. 8,575,381, 2013.

(16) Teichmann, J.; Wagner, M. Silicon Chemistry in Zero to Three Dimensions: From Dichlorosilylene to Silafullerane. *Chem. Commun.* **2018**, *54* (12), 1397–1412.

(17) Eger, W. A.; Genest, A.; Rösch, N. Thermal Decomposition of Branched Silanes: A Computational Study on Mechanisms. *Chem. - Eur. J.* **2012**, *18* (29), 9106–9116.

(18) Swihart, M. T.; Girshick, S. L. Ab Initio Structures and Energetics of Selected Hydrogenated Silicon Clusters Containing Six to Ten Silicon Atoms. *Chem. Phys. Lett.* **1999**, *307* (July), 527–532.

(19) Swihart, M. T.; Girshick, S. L. Thermochemistry and Kinetics of Silicon Hydride Cluster Formation during Thermal Decomposition of Silane. *J. Phys. Chem. B* **1999**, *103*, 64.

(20) Swihart, M. T. Electron Affinities of Selected Hydrogenated Silicon Clusters (SixHy, $x = 1-7$, $y = 0-15$) from Density Functional Theory Calculations. *J. Phys. Chem. A* **2000**, *104* (25), 6083–6087.

(21) Martin, J. G.; O'Neal, H. E.; Ring, M. A. Thermal Decomposition Kinetics of Polysilanes: Disilane, Trisilane, and Tetrasilane. *Int. J. Chem. Kinet.* **1990**, *22* (6), 613–631.

(22) Shinohara, M.; Maehama, T.; Niwano, M. Adsorption and Decomposition of Methylsilanes on Si(100). *Appl. Surf. Sci.* **2000**, *162-163*, 161–167.

(23) Arkles, B.; Pan, Y.; Kaloyeros, A. E. Thin Film Deposition of Silicon Nitrides and Oxides from Trihydrosilanes. *ECS Trans.* **2014**, *64* (9), 243–249.

(24) Jasinski, J. M. Gas Phase and Gas Surface Kinetics of Transient Silicon Hydride Species. In *Material Research Society Proceedings*; Montziariaris, T. J., Paz-Pujalt, G. R., Smith, F. T. J., Westmoreland, P. R., Eds.; Materials Research Society: 1994; Vol. 334, pp 11–18.

(25) Walsh, R. In *Silicon Compounds: Silanes and Silicones*; Arkles, B. C., Larson, G. L., Eds.; Gelest: 2008; pp 200–207.

(26) Wu, Y.; Wong, C. Substituent Effect on the Dissociation Energy of the Si-H Bond: A Density Functional Study. *J. Org. Chem.* **1995**, *60*, 821–828.

(27) Lu, X.; Anderson, K. J.; Boudjouk, P.; Korgel, B. Low Temperature Colloidal Synthesis of Silicon Nanorods from Isotetrasilane, Neopentasilane, and Cyclohexasilane. *Chem. Mater.* **2015**, *27*, 6053–6058.

(28) Hazbun, R.; Hart, J.; Hickey, R.; Ghosh, A.; Fernando, N.; Zollner, S.; Adam, T. N.; Kolodzey, J. Silicon Epitaxy Using Tetrasilane at Low Temperatures in Ultra-High Vacuum Chemical Vapor Deposition. *J. Cryst. Growth* **2016**, *444*, 21–27.

(29) Chung, K. H.; Yao, N.; Benziger, J.; Sturm, J. C.; Singh, K. K.; Carlson, D.; Kuppuraio, S. Ultrahigh Growth Rate of Epitaxial Silicon by Chemical Vapor Deposition at Low Temperature with Neopentasilane. *Appl. Phys. Lett.* **2008**, *92* (11), 113506.

■ NOTE ADDED AFTER ASAP PUBLICATION

This paper was published on the Web on February 20, 2019. Additional text corrections were implemented, and the corrected version was reposted on February 21, 2019.